

Award Number: W81XWH-07-1-0247

TITLE: Transrectal Near-Infrared Optical Tomography for Prostate Imaging

PRINCIPAL INVESTIGATOR: Daqing Piao, Ph.D.

CONTRACTING ORGANIZATION: Oklahoma State University  
Stillwater, OK 74078

REPORT DATE: March 2008

TYPE OF REPORT: Annual

PREPARED FOR: U.S. Army Medical Research and Materiel Command  
Fort Detrick, Maryland 21702-5012

DISTRIBUTION STATEMENT: Approved for Public Release;  
Distribution Unlimited

The views, opinions and/or findings contained in this report are those of the author(s) and should not be construed as an official Department of the Army position, policy or decision unless so designated by other documentation.

# REPORT DOCUMENTATION PAGE

*Form Approved*  
*OMB No. 0704-0188*

Public reporting burden for this collection of information is estimated to average 1 hour per response, including the time for reviewing instructions, searching existing data sources, gathering and maintaining the data needed, and completing and reviewing this collection of information. Send comments regarding this burden estimate or any other aspect of this collection of information, including suggestions for reducing this burden to Department of Defense, Washington Headquarters Services, Directorate for Information Operations and Reports (0704-0188), 1215 Jefferson Davis Highway, Suite 1204, Arlington, VA 22202-4302. Respondents should be aware that notwithstanding any other provision of law, no person shall be subject to any penalty for failing to comply with a collection of information if it does not display a currently valid OMB control number. **PLEASE DO NOT RETURN YOUR FORM TO THE ABOVE ADDRESS.**

<b>1. REPORT DATE (DD-MM-YYYY)</b> 01-03-2008			<b>2. REPORT TYPE</b> Annual		<b>3. DATES COVERED (From - To)</b> 1 MAR 2007 - 28 FEB 2008	
<b>4. TITLE AND SUBTITLE</b>  Transrectal Near-Infrared Optical Tomography for Prostate Imaging					<b>5a. CONTRACT NUMBER</b>	
					<b>5b. GRANT NUMBER</b> W81XWH-07-1-0247	
					<b>5c. PROGRAM ELEMENT NUMBER</b>	
<b>6. AUTHOR(S)</b> Daqing Piao, Ph.D.  E-Mail: daqing.piao@okstate.edu					<b>5d. PROJECT NUMBER</b>	
					<b>5e. TASK NUMBER</b>	
					<b>5f. WORK UNIT NUMBER</b>	
<b>7. PERFORMING ORGANIZATION NAME(S) AND ADDRESS(ES)</b>  Oklahoma State University Stillwater, OK 74078					<b>8. PERFORMING ORGANIZATION REPORT NUMBER</b>	
<b>9. SPONSORING / MONITORING AGENCY NAME(S) AND ADDRESS(ES)</b> U.S. Army Medical Research and Materiel Command Fort Detrick, Maryland 21702-5012						
<b>10. SPONSOR/MONITOR'S ACRONYM(S)</b>					<b>11. SPONSOR/MONITOR'S REPORT NUMBER(S)</b>	
<b>13. SUPPLEMENTARY NOTES</b>						
<b>14. ABSTRACT</b> The objective of this research is to explore the technology of trans-rectal near-infrared (NIR) optical tomography for accurate, selective prostate biopsy. The research in the first year has made several key advancements that may render future testing of the approach at in vivo settings. The development of a 20mm diameter axial-imaging cylindrical applicator for trans-rectal NIR optical tomography represents an unprecedented engineering approach in the development of internal-imaging NIR tomography applicator. Simulations and experiments both demonstrated the feasibility of imaging target with absorption contrast by use of trans-rectal NIR tomography applicator, even though the interrogation depth may be limited to ~15mm. The findings from a trans-rectal NIR probe having elliptical cross-section gives an option of potentially imaging deeper tissue volumes up to 20mm at axial-imaging geometry.						
<b>15. SUBJECT TERMS</b> No subject terms provided.						
<b>16. SECURITY CLASSIFICATION OF:</b>				<b>17. LIMITATION OF ABSTRACT</b>	<b>18. NUMBER OF PAGES</b>	<b>19a. NAME OF RESPONSIBLE PERSON</b> USAMRMC
<b>a. REPORT</b> U	<b>b. ABSTRACT</b> U	<b>c. THIS PAGE</b> U	UU			29

## Table of Contents

	<u>Page</u>
<b>Introduction.....</b>	<b>01</b>
<b>Body.....</b>	<b>01</b>
<b>Key Research Accomplishments.....</b>	<b>13</b>
<b>Reportable Outcomes.....</b>	<b>14</b>
<b>Conclusion.....</b>	<b>15</b>
<b>References.....</b>	<b>15</b>
<b>Appendices.....</b>	<b>16</b>

# **ANNUAL REPORT**

## **PCRP 060814----“Transrectal Near-Infrared Optical Tomography for Prostate Imaging”**

### **INTRODUCTION**

The objective of this research is to explore the technology of trans-rectal near-infrared (NIR) optical tomography for accurate, selective prostate biopsy. Prostate cancer is the most common non-dermatologic cancer in American men. Prostate cancer suspicion is typically based on an elevated serum prostate-specific antigen (PSA) level or a suspicious nodule found during a digital rectal exam (DRE). When the PSA level is elevated or the DRE shows abnormal, there is a 25 % chance that cancer is present. The existence of prostate cancer can only be confirmed by a needle biopsy that is guided by trans-rectal ultrasound (TRUS). Since there are no pathognomonic findings for prostate cancer on ultrasound imaging, random biopsies are taken systematically throughout the prostate. The accuracy of biopsy is problematic and many men undergo multiple biopsies due to the lack of a more specific/sensitive imaging modality. Pathologic studies have demonstrated increased vasculature associated with prostate cancer, as well as a positive correlation between micro-vessel density and the aggressiveness of the disease. Near-infrared (NIR) optical tomography is known of sensitive to vascular-based contrast, therefore trans-rectally implemented NIR optical tomography may provide a new way of assessing the prostate cancer. One of the outcomes of trans-rectal NIR tomography of the prostate will be a more accurate imaging guidance for targeted prostate biopsy.

### **BODY**

#### **1. Proposed Specific Aims:**

- (1) To demonstrate that endoscopic NIR tomography at a probe size of 25mm in diameter can be achieved by use of spread-spectral-encoding from a broad-band light source.
- (2) To demonstrate that trans-rectal NIR tomography can image the prostate at the proximity of the rectum with significant tumor-tissue contrast.
- (3) To demonstrate that multi-spectral trans-rectal NIR tomography can be implemented with the single trans-rectal imaging probe.
- (4) To demonstrate that trans-rectal multi-spectral NIR tomography can quantify the hemoglobin concentration and oxygenation saturation in phantom, and further in prostate tumor model if the time of research allows.

#### **2. Progress on Specific Aim 1**

##### ***2.1 Development of an applicator for trans-rectal NIR optical tomography***

A 25mm diameter trans-rectal NIR tomography probe for axial imaging was proposed in the research. With more discussions and feedback from prostate cancer physician, we decided that a 20mm diameter axial-imaging applicator for trans-rectal NIR tomography would be developed. This probe dimension change was attributed to the fact that commercial trans-rectal ultrasound (TRUS) transducers typically have a size of 20mm in diameter. A 20mm trans-rectal NIR probe

will facilitate better ways of comparing with TRUS and would be more comfortable for patients if tested clinically.

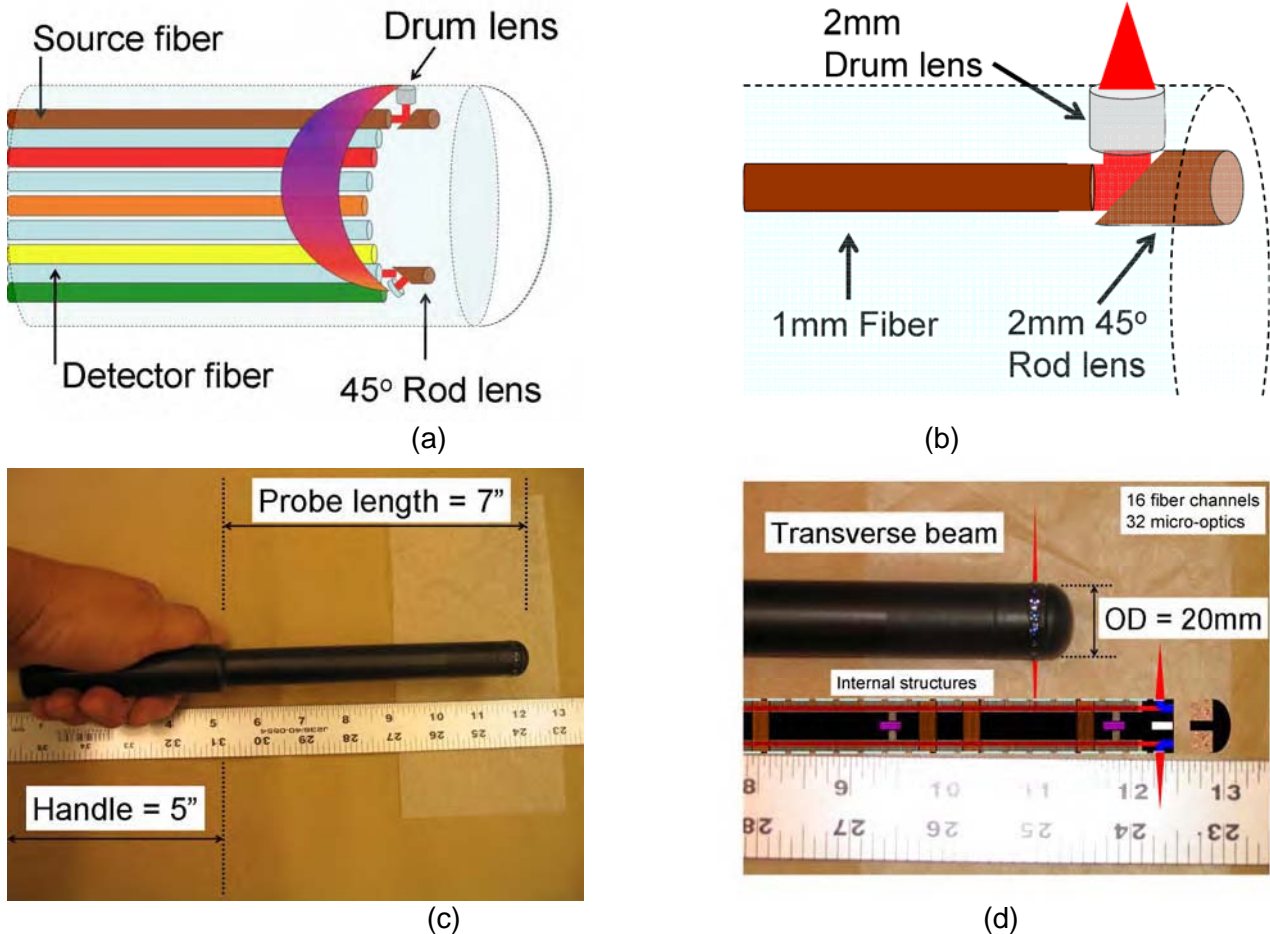


Figure 1. The 20mm axial-imaging applicator for trans-rectal NIR tomography. (a) Illustration of the fiber arrangement inside the applicator. (b) Each source/detector channel consists of a 1mm bare fiber, a 45° rod lens of 2mm in diameter, and a drum lens of 2mm in diameter. The configuration allows side-firing for axial-imaging. (c) Photograph of the probe, where the length of the probe is given. (d) Photograph of the distal part of the probe, where the micro-optics components (drum lenses) with anti-reflection coating are shown and the internal structure of the probe is also sketched.

The fabrication method described previously in the research proposal for the 25mm diameter probe was applied to the development of this 20mm axial-imaging trans-rectal NIR tomography applicator. The design and fabrication details of this 20mm trans-rectal NIR applicator are given in Fig. 1. Sixteen bare fibers of 1.0mm core diameter are evenly spaced on a circle by having source and detector channel interspersing with each other, as shown in Fig. 1(a). Each fiber is parallel to the probe axis, and is aligned to a 45° rod lens of 2mm in diameter to deflect the beam 90° for side-firing. A 2mm diameter drum lens is then used to provide a sealed optical aperture for illumination as well as beam focusing, as shown in Fig. 1(b). Photographs of this applicator are presented in Fig. 1(c) and (d), where it can be seen that the applicator part having the NIR array is 7" long, and the handle part is 5" long. Inside the applicator, there are 4 guiding platforms to maintain the alignment of the fiber in a long distance. Each of the guiding platforms has 16 evenly spaced holes on a circle. The most complicated

part is the module holding the distal end of the fiber and the 32 micro-optics components. The chambers of the fiber, rod lens, and drum lens have been fabricated in a way to assure accurate alignment of each channel. The fiber has been individually polished and placed in the housing module. The orientation of the 45° rod lens is aligned using another 45° rod lens in the place of the drum lens by matching the hypertension surface, and finally the drum lens is placed. All the fibers, rod lenses, and drum lenses are secured with UV-curing epoxy. Among these 16 optical channels, it has been found that the source channel 5 has slight miss-alignment of the rod lens with respect to the side-firing geometry, but our method [1-2] was able to compensate the non-uniformity.

The 8 channels of source fibers are grouped to a 3-meter long fiber cable, and distributed as a linear fiber bundle at the proximal end of the cable (see Fig. 2). The linear source fiber bundle couples different spectral-components of a broad-band superluminescent diode by use of spread-spectral-encoding configuration [1]. The 8 channels of detection fibers are also grouped to a 3-meter long fiber cable and distributed linearly at the proximal end. The linear detector fiber bundle is aligned vertically to the entrance slit of a spectrometer. The signals from different source channels are separated horizontally by spectral-decoding and the vertical positions of the fiber at the spectrometer imaging plane differentiate the detection channel [3, 4]. A 16bit CCD camera acquires the 2-D signals corresponding to all source and detector pairs.



Figure 2. Photographs of the 20mm axial-imaging trans-rectal NIR applicator including the fiber cable (a) and the complete NIR scanner assembled on a custom-cart (b).

## **2.2 Preliminary sensitivity studies of transrectal NIR optical tomography by use of the 20mm applicator**

### **2.2.1 Simulation geometry**

Trans-rectal NIR tomography in an axial-imaging geometry is potentially different from all NIR tomography approaches investigated previously for breast or brain imaging applications. The differences lie in at least three aspects: (1) The array geometry is in a hollow annular shape where the source/detectors are in the inner region of the targeted medium. For closer source-detector pairs, a semi-infinite boundary condition may be valid; for source-detector located at the opposite sides of the array, the photon path might not be deep enough to sense the tissue

medium. (2) The distances of closest source & detector may be comparable to the mean scattering path-length. (3) Targets close to the probe-tissue interface may need to be reconstructed. Therefore it is understood that a diffusion approximation to the radiative transfer equation that is conventionally employed in NIR tomography may not be valid everywhere for this axial trans-rectal imaging geometry. Nevertheless, the diffusion approximation is a manageable approximation and it will be a good starting point to understand the qualitative aspects of this new axial trans-rectal imaging geometry.

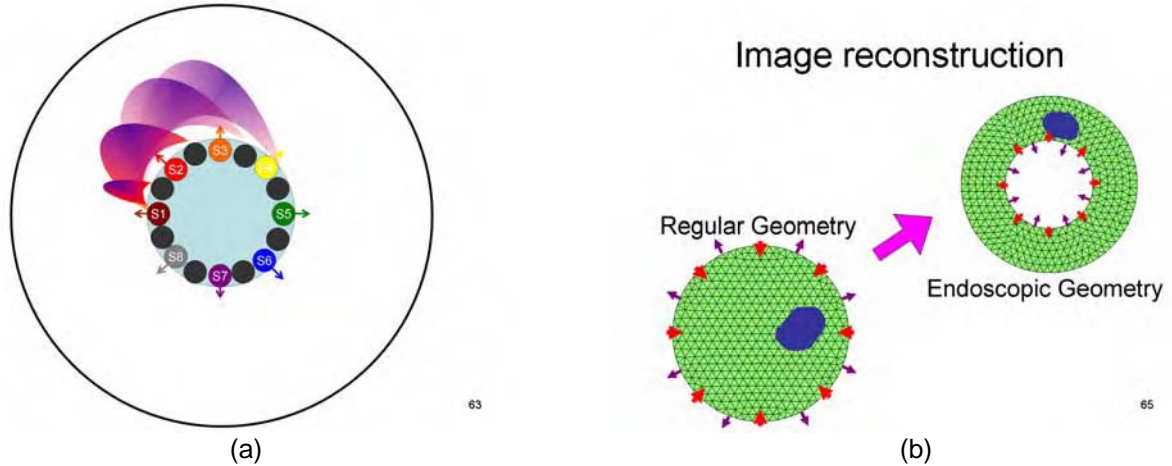


Figure 3. The transversal transrectal imaging geometry and the necessary mesh modification for the forward/inverse problem form a typical external imaging geometry like that of breast.

We used NIRFAST [5] modeling package to investigate axial-imaging trans-rectal NIR tomography. NIRFAST package was developed in Dartmouth College for frequency-domain reconstruction based on finite-element solution of diffusion equation, and it was used by several groups for conventional NIR tomography systems where the fiber arrays typically have ring-type geometry for imaging the internal volume. In axial-imaging trans-rectal NIR tomography the imaging geometry is flipped inside-out (shown in Fig. 3(a)), therefore a hollow-centered circular mesh (shown in Fig. 3(b)) becomes the first modification we implemented in NIRFAST. Relevant modifications have been made to adjust the program in accordance with the axial trans-rectal imaging geometry.

The simulation using NIRFAST is conducted for frequency-domain even though our current imager is in CW mode. The forward problem is solved by finite element method, and the absorption and scattering properties is reconstructed by a Levenberg-Marquardt iterative solver. The imaging field-of-view in the simulation is set to be 20mm from the probe surface (60mm in diameter for the entire volume). In all simulations 1% Gaussian-distributed zero mean noise has been added to the source-detector forward data. The size of an inclusion target is set to 7.7mm in diameter. The background optical properties are set to  $\mu_a = 0.002mm^{-1}$  and  $\mu_s' = 0.5mm^{-1}$  for comparison with experimental measurements using a 5% intralipid solution.

### 2.2.2 Depth-dependent detection sensitivity profile

It is known that the accuracy of the image reconstruction is dependent upon many factors, including the mesh size [6]. The biggest mesh that NIRFAST can handle has 40674 nodes; however, it is not desirable to use the 40674-node mesh for reconstruction investigations since

it is too time-consuming as it requires over 500 seconds calculating the Jacobian and at least 7.6 GB of memory. A balance between computation time and accuracy needs to be determined to find the optimum mesh size for image reconstruction study. One method to evaluate the accuracy of the mesh, in the case of NIRFAST, is to compare the Jacobian matrix values between two meshes of different densities at each node. To compare the Jacobian values, the sum of all source-detector measurements were normalized with respect to the element areas of each mesh. Then, using a modified approach from Yalavarthy [6], the normalized Jacobian values were interpolated to a 60mm×60mm grid with 0.25mm spacing. Figure 4 shows a plot of the normalized, interpolated Jacobian values for the 40674 node mesh. For comparison, the

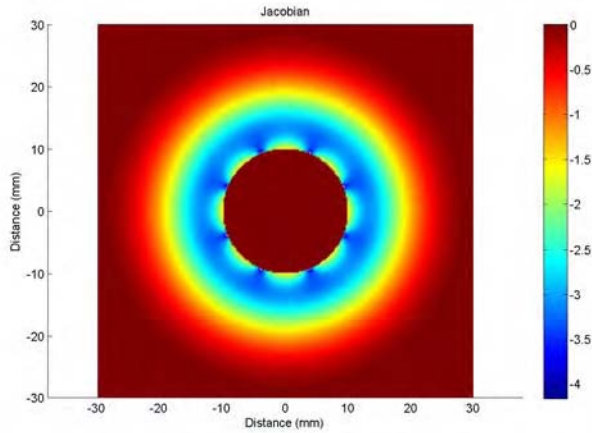


Figure 4. Plot of the Jacobian values summed over all source-detector measurements

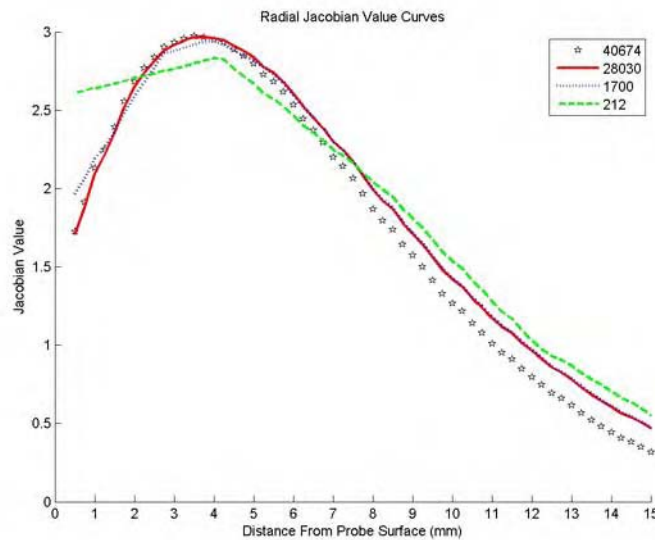


Figure 4. Jacobian values along radial line from probe surface for different mesh sizes

Jacobian values were extracted along a 2 degree radial slice at 0.25mm intervals from the probe surface to the outer boundary. A qualitative analysis of the Jacobian values can be obtained from Fig. 4. For small mesh sizes, the Jacobian values are drastically different from the reference, especially near the probe surface. There is little difference between the 1700 and 28030 meshes as compared to the mesh of 40674; however, a mesh size of only 212 isn't. A

quantitative analysis of the error and computation time is conducted to determine the optimum mesh size for further studies.

### 2.2.3 Optimum mesh size

The difference between the curves of varying mesh sizes were quantified by computing the RMS value of the difference between each mesh and the reference by [6]

$$RMS\_error = \sqrt{\frac{1}{N} \sum_{i=1}^N (J_{test,i} - J_{reference,i})^2} \quad (1)$$

Table. 1. Error between Jacobian matrices for various mesh sizes compared to the reference mesh

Mesh Size	RMS Error	Error Decrease	Jacobian Computation Time (s)	Time Factor Increase from Previous Mesh Size
<b>28030</b>	0.11528	0.0002	107.40	1.57
<b>20795</b>	0.11549	0.0009	68.47	2.85
<b>10284</b>	0.11634	0.0009	24.05	1.39
<b>8061</b>	0.11726	-0.0001	17.34	1.29
<b>6619</b>	0.11713	0.0047	13.40	4.64
<b>3291</b>	0.1218	0.0008	2.89	1.42
<b>2628</b>	0.12264	0.0059	2.04	1.62
<b>1700</b>	0.12858	0.0138	1.26	1.48
<b>1165</b>	0.14233	0.0069	0.85	1.42
<b>856</b>	0.14926	0.0165	0.60	1.07
<b>685</b>	0.16579	0.0175	0.56	1.70
<b>495</b>	0.18328	0.0245	0.33	1.32
<b>361</b>	0.20781	0.0293	0.25	1.04
<b>287</b>	0.23714	0.0192	0.24	1.60
<b>212</b>	0.25637		0.15	

Where N is the number of values within the radial Jacobian values,  $J_{test,i}$  is the  $i$ -th value of the test Jacobian value, and  $J_{reference,i}$  is the  $i$ -th value of the reference Jacobian. The value from equation (1) is a measure of the average difference between the reference Jacobian and the Jacobian under test. The Jacobian calculation is almost the most time consuming calculation during reconstruction, thereby is used for speed comparisons. Table 1 lists the RMS

error to the reference mesh and Jacobian calculation times for each mesh size. Figure 5 plots the RMS error values as a function of mesh size to visualize the data in Table 1. The “time factor increase” in Table 1 is calculated by dividing the current mesh size computation time by the previous mesh size computation time.

It is found from Table 1 or Fig. 5 that the total error decrease for node sizes above 1700 to 28030 is not as much as the error decrease from 1165 nodes to 1700 nodes; furthermore the calculation time for the 2628 node mesh is nearly twice the time as the 1700 node mesh, while the time factor increase between mesh sizes below 1700 nodes is nearly 1.50. Therefore, the 1700 node mesh is chosen for further simulative studies as it gives a good balance between accuracy and computation time.

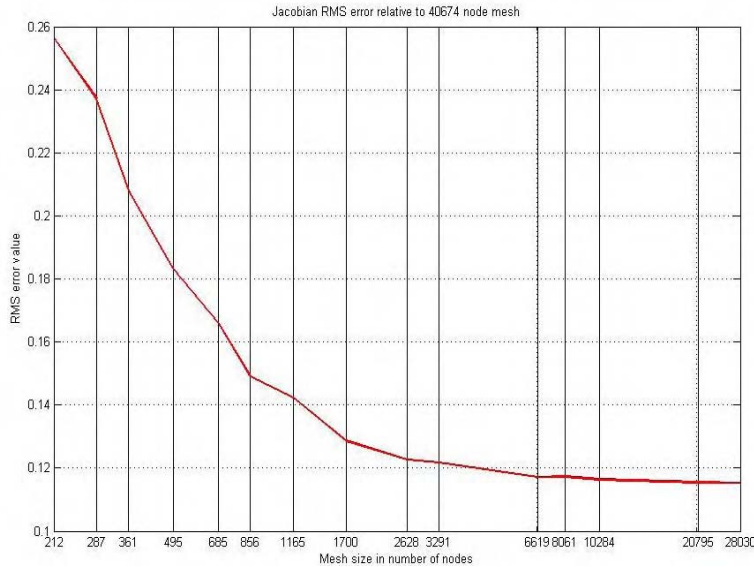


Figure 5 Plot of the RMS error values in table 1

### 2.3 Simulative image reconstruction studies of transrectal NIR optical tomography by use of the 20mm applicator

One of the most critical parameters in axial-imaging trans-rectal NIR tomography may be the imaging depth that it can achieve. Using the mesh size of 1700 nodes suggested by previous investigations, different contrast levels with respect to the background absorption coefficient were evaluated to determine the maximum depth the phantom is detectable: first a 100X contrast target is used to simulate an infinite absorbing phantom, and a 3X contrast is used to simulate a tumor-like lesion. All distances are quoted as the distance from the center of the inclusion target to the surface of the probe.

#### 2.3.1 Imaging targets having infinite absorption contrast

The absorption coefficient of the infinite contrast target is set at 0.2mm<sup>-1</sup>, and the reduced scattering coefficient value is maintained at the background value of 0.5mm<sup>-1</sup>. Figure 6 shows the variability of the maximum reconstructed  $\mu_a$  values as a function of distance between the target center to the probe surface. The general decrease in reconstructed  $\mu_a$  values is to be expected, since as the target is moved away from the probe’s surface, the Jacobian value decreases.

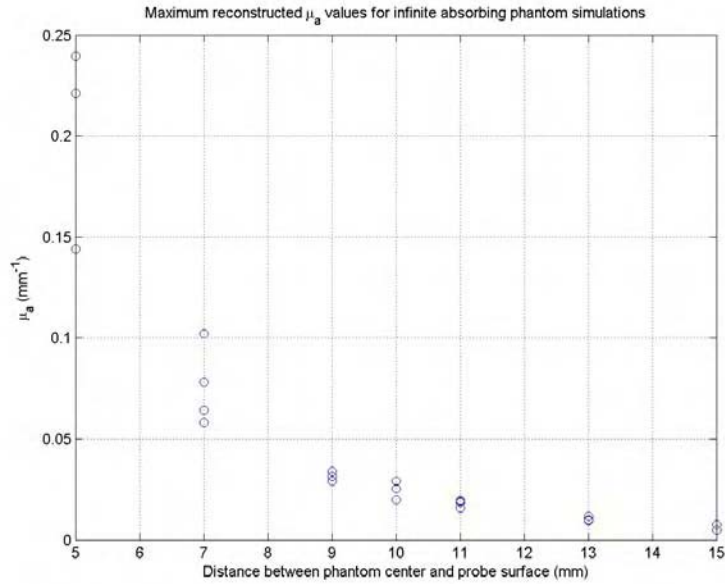


Figure 6 Plot of the maximum reconstructed  $\mu_a$  value for each reconstructed infinite absorbing phantom image plotted by distance between center of phantom and surface of the probe.

The reconstructed images for target depths of 5, 10, and 15mm are displayed in Fig. 7. It is indicated from Fig. 7 that a strong absorbing target at depth up to 15mm may be reconstructed at the correct azimuth direction, but with less accurate depth localization. The error in the depth location is apparently related to the decrease of the sensitivity along the depth, which tends to reconstruct the target at the highest sensitivity location [7].

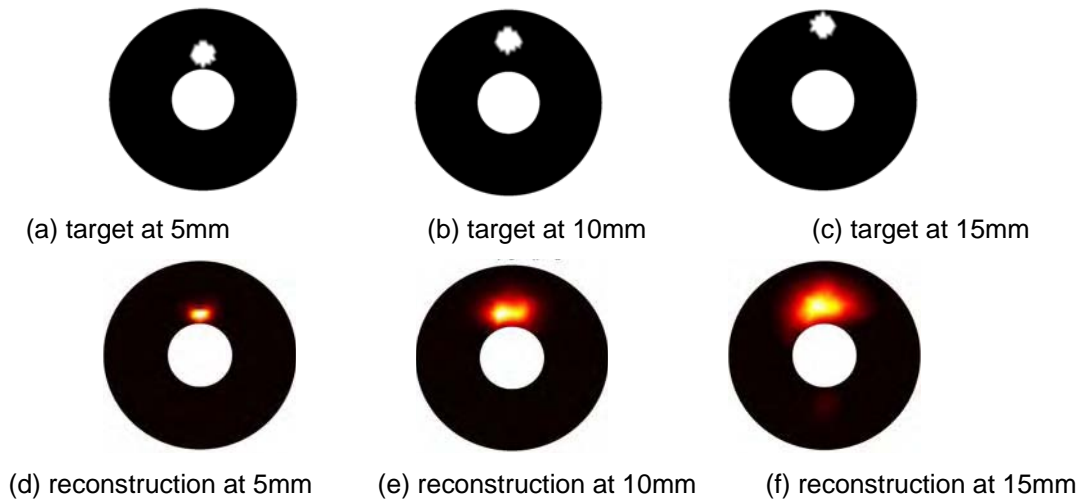


Figure 7 Reconstructed Images for the infinite phantom case. (a)-(c) Phantom locations. (d)-(f) Reconstructed images.

### 2.3.2 Imaging targets having 3 folds of absorption contrast

The tissue-like phantom properties were set at  $\mu_a = 0.0059\text{mm}^{-1}$  and  $\mu_s' = 1.03\text{mm}^{-1}$ , which are the properties of a phantom available in the experiment. The variability of the maximum

reconstructed  $\mu_a$  value was also measured for this phantom at various distances and plotted in Figure 8. Although the values for each distance are not as consistent as the infinite phantom case, there appears to be some reduction in the average maximum reconstructed  $\mu_a$  values as distance increases. Figure 9 shows the reconstructed images for various depths of the tissue-like phantom. As with the infinite phantom case, the reconstructed tissue-like phantom appears within the region with a high Jacobian value (~5mm from the probe surface). The azimuthal location cannot be correctly determined as deep as the infinite case, but is determinable up to 7mm.

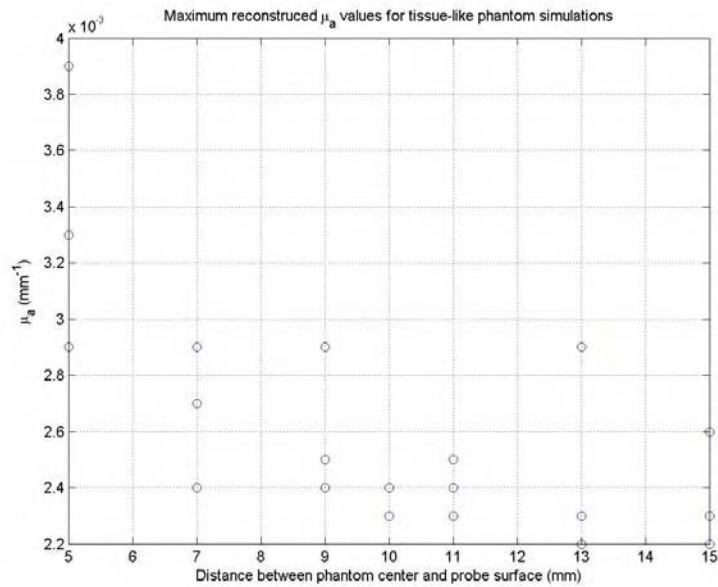


Figure 8. Plot of the maximum reconstructed  $\mu_a$  value for each reconstructed tissue-like phantom image plotted by distance between center of phantom and surface of the probe.

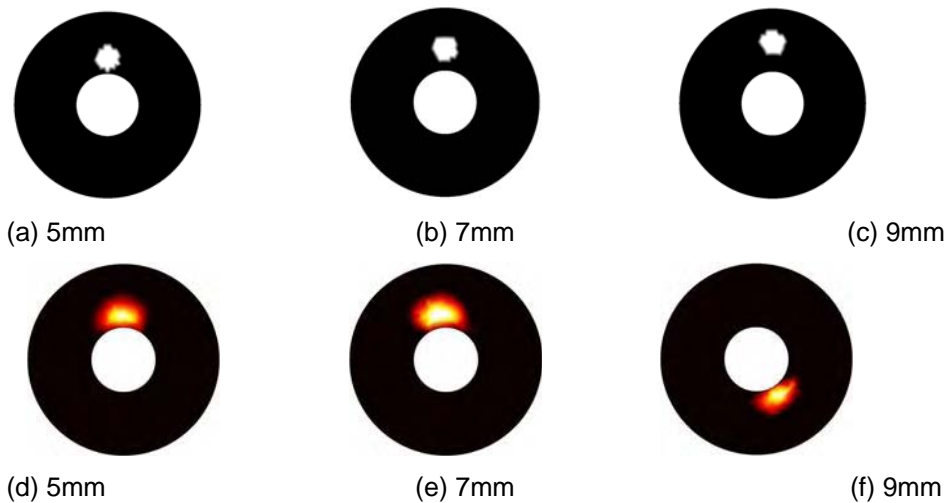


Figure 9. Reconstructed images for the tissue-like phantom. (a)-(c) Phantom locations. (d)-(f) Reconstructed images.

## 2.4 Experimental phantom studies of transrectal NIR optical tomography by use of the 20mm applicator

Phantom experiments have been conducted to validate the findings of numerical simulations. A 0.5% bulk Intralipid solution was set as the background. A black absorbing rod of 8mm diameter was used to emulate an infinite absorbing target. A linear translation stage held the rod in parallel to the TR-NIR probe, and moved the rod away from the probe from 5mm depth at an increment of 1mm, up to 20mm. The reconstructed images in Figure 10 show that the strong absorbing target may be imaged at a depth greater than 13mm; however, the overall accuracy of depth localization is low.

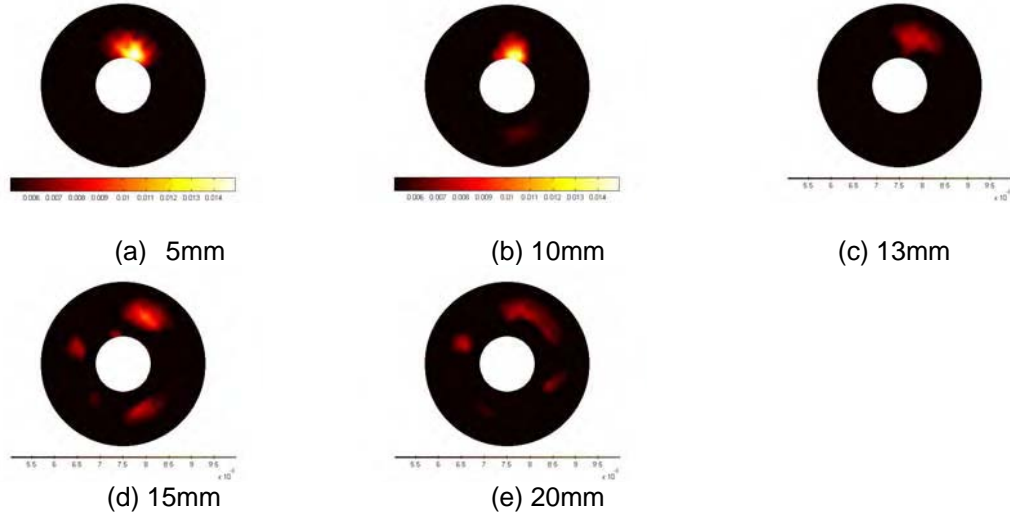


Figure 10. Experimental results for an 8mm blob of black absorbing rod in a 0.5% Intralipid solution. (a) Target depth of 5mm. (b) Target depth of 10mm. (c) Target depth of 13mm. (d) Target depth of 15mm. (e) Target depth of 20mm.

Similar experiments were repeated for the solid phantom of 7.8mm diameter having  $\mu_a = 0.0059\text{mm}^{-1}$  and  $\mu_s' = 1.03\text{mm}^{-1}$  used to simulate a 3x contrast target. The images are shown in Fig. 11, where the blob at depth of 7mm can be reconstructed. However, considerable artifacts appear for blob depth at or above 9mm. The phantom experimental results agree with the prediction by the numerical simulations, and both justify the need of a rigorous investigation of the forward modeling for this endoscopy NIR geometry or a method of compensating the degrading sensitivity along the depth.

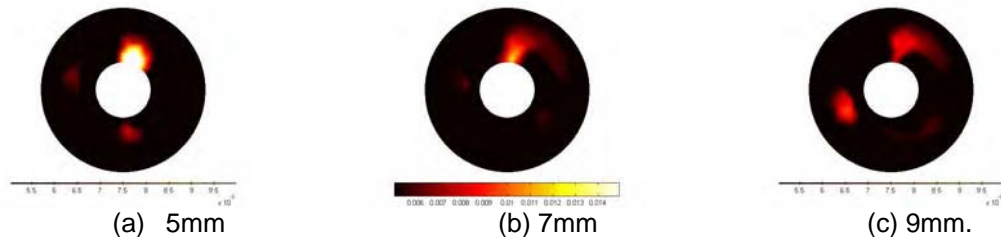
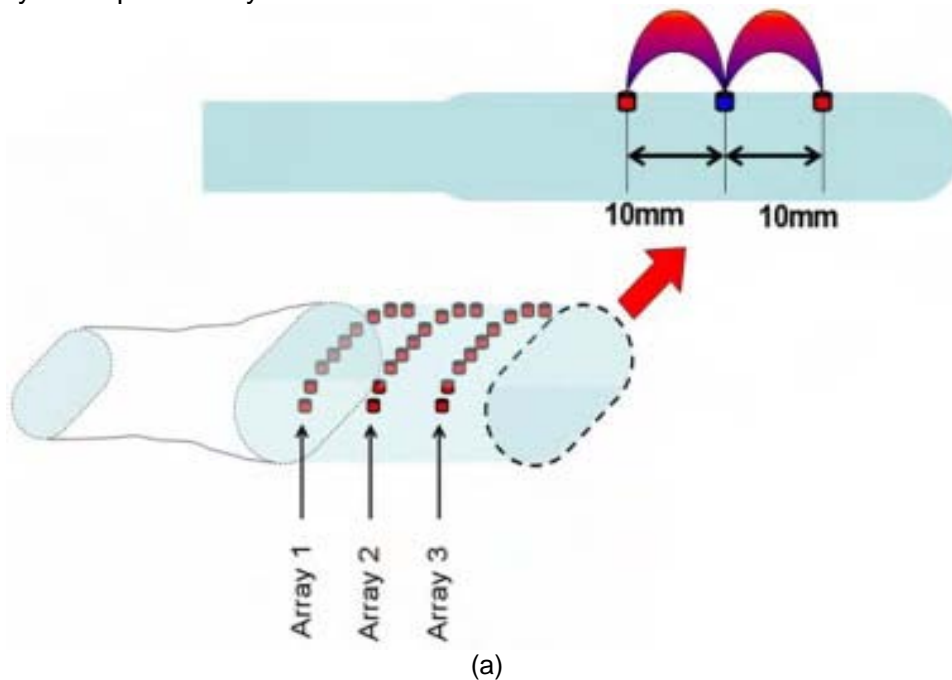
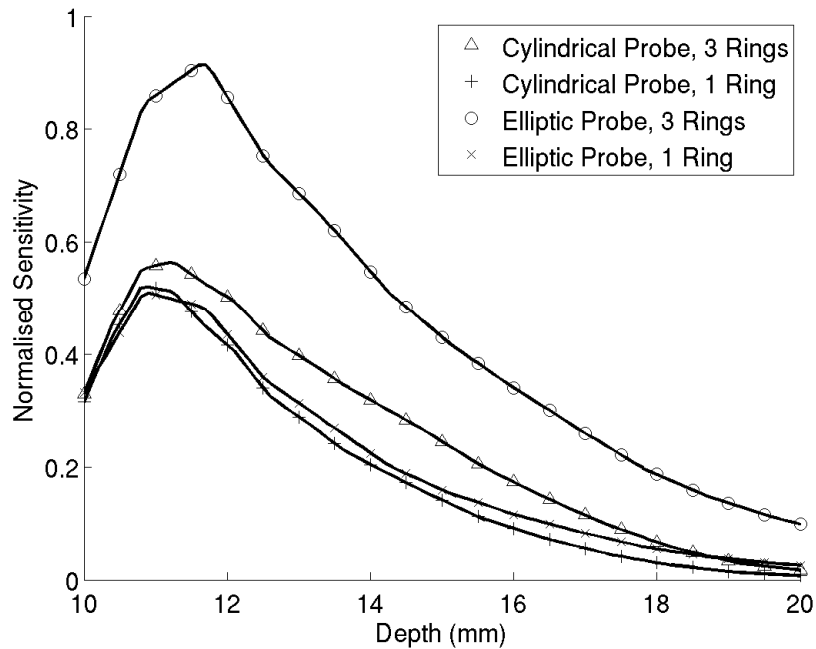


Figure 11. Experimental results for a 7.8mm blob of ~3x contrast in a 0.5% Intralipid solution. (a) Target depth of 5mm. (b) Target depth of 7mm. (c) target depth of 9mm.

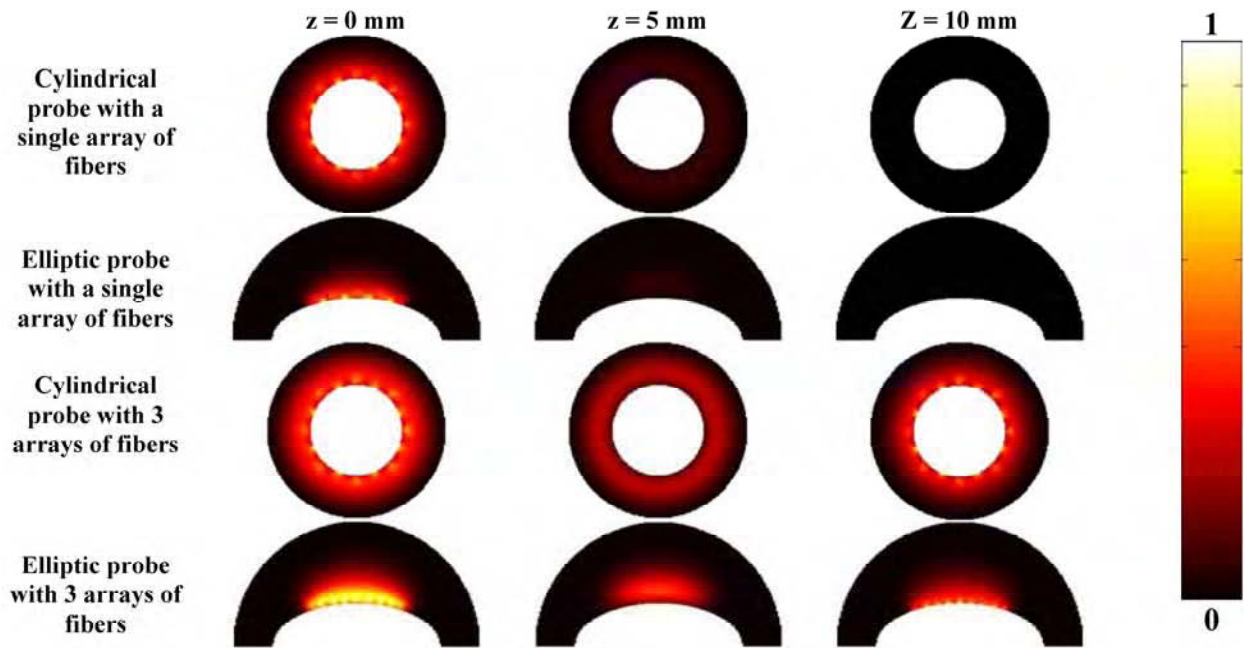
## 2.5 Simulation studies of transrectal NIR optical tomography by use of an applicator having elliptical cross-section

The previous simulation and experimental studies have found that the 20mm trans-rectal NIR probe is capable of imaging target at a depth of ~15mm for highly absorbing target and ~7mm for lower contrast target. It is speculated that the circularly symmetric arrangement of optodes has limited the imaging depth of this probe, therefore we also investigated a side-firing NIR probe geometry having an elliptical cross-section with single or multiple layers of NIR arrays. The shape of the probe is shown in Fig. 12 (a), where the probe cross-section is elliptical and 2 arrays of optodes are included, with one detector array in the center and 2 source arrays run parallel to the detector array at 10mm separation. The probe is an elliptical cylinder of length 40mm with major radius 20mm and minor radius of 10mm. The three arrays have a longitudinal separation of 10mm and placed along the minor axes at positions  $z = -10$  mm,  $z = 0$  mm and  $z = 10$  mm about  $x = 0$  mm. Two different data collection strategies are considered: (1) 5 sources and 4 detectors interleaved in a single line (Array 2 in Fig. 12(a)), and (2) three separate rings of 8 sources (Array 2) at  $z=0$ mm and 8 detectors (Array 1 and 3) at  $z = 10$  mm and  $-10$  mm. The sensitivity studies in (b) and (c) reveal that when the cross-sections of a circular and elliptical probes are comparable to each other, the elliptical-shape probe can interrogate target of 20mm deep [8]. This study indicates that transversal imaging of prostate peripheral zone beyond 2cm is feasible by an elliptical array.





(b)



(c)

Figure 12. (a) Design of an elliptical probe. (b) Comparison of normalized cross-sectional sensitivity profiles of cylindrical and elliptic probes. (c) The normalized sensitivity of each probe design and fiber arrangement strategy. The images presented are coronal cross-sections of the probe at different sections. Note that for the cylindrical case the depth of tissue modeled as surrounding the probe is set at 10 mm, whereas in the elliptic case the depth of tissue surrounding the probe is set at 20 mm in the short axis and 10 mm in the long axis.

In order to further analyze the depth sensitivity of the measurements with respect to absorption changes within the surrounding tissue, simulated data was generated for the elliptical probe, assuming either a single array or three array of fibers. A small 5 mm diameter anomaly with 3 times the background absorption was placed at either 6 or 8 mm depth within the tissue and intensity only data was simulated using NIRFAST with 1% noise. The results in Fig. 13 demonstrate the improvement of imaging depth as well as the depth localization using this elliptical probe when compared with the previous circular probe. An elliptical probe may be fabricated to validate these findings from experiments.

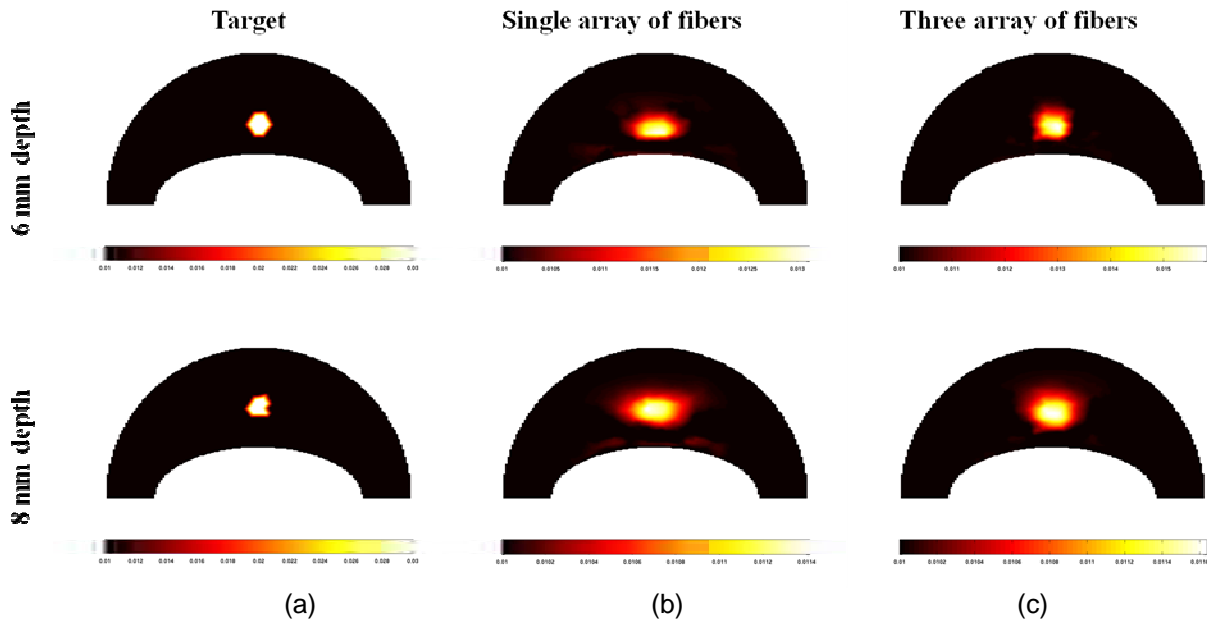


Figure 13. Reconstructed tomographic absolute images of absorption using simulated data for the elliptical probe. The images presented are coronal cross-sections of the 3D model at  $z = 0$  mm. (a) target setting. (b) Reconstructions using single array in the  $Z=0$ . (c) Reconstructions using 3 arrays of fibers.

## KEY RESEARCH ACCOMPLISHMENTS

The following research accomplishments have been made during the first year of this project:

1. Developed a 20mm diameter axial-imaging cylindrical applicator for trans-rectal NIR optical tomography. The design and fabrication procedures were validated. The use of micro-optics in the fabrication of this trans-rectal NIR tomography represents an unprecedented approach in the development of NIR tomography applicator for use in restricted space, and may set as a template for future instrumentation of NIR diffuse optical tomography probes for imaging of other internal organs.
2. Conducted simulations to investigate the imaging performance of this 20mm trans-rectal NIR applicator. The sensitivity of this cylindrical probe having one array of interspersed source and detector channels is found to degrade rather rapidly along the depth. For target of highly absorbing contrast, it may be reconstructed at depth up to  $\sim 15$ mm, while for target of lower absorption contrast, it may be detected at depth within 10mm.



2. Musgrove, Cameron H. MS degree granted on Dec. 2007.  
Employed in Sandia National Lab
3. XIE, Hao MS student

**Proposals Submitted To:**

1. National Science Foundation (PI) \$515,669 submitted on 07/18/2007  
CAREER: Transrectal optical tomography and ultrasound for prostate imaging  
Status: declined
2. National Institutes of Health (PI) \$3,568,228 submitted on 02/05/2008  
Integrated trans-rectal near-infrared and ultrasound system for prostate cancer imaging  
Status: pending

**CONCLUSIONS**

The objective of this research is to explore the technology of trans-rectal near-infrared (NIR) optical tomography for accurate, selective prostate biopsy. The research in the first year has made several key advancements that may render future testing of the approach at in vivo settings. The development of a 20mm diameter axial-imaging cylindrical applicator for trans-rectal NIR optical tomography represents an unprecedented engineering approach in the development of internal-imaging NIR tomography applicator. Simulations and experiments both demonstrated the feasibility of imaging target with absorption contrast by use of trans-rectal NIR tomography applicator, even though the interrogation depth may be limited to ~15mm. The findings from a trans-rectal NIR probe having elliptical cross-section gives an option of potentially imaging deeper tissue volumes up to 20mm at axial-imaging geometry.

**REFERENCES**

1. Piao D, Xie H, Zhang W, Kransinski JS, Zhang G, Dehghani H, and Pogue BW, "Endoscopic, rapid near-infrared optical tomography", *Optics Letters*, Vol. 31, No. 19, pp. 2876-2878 (2006).
2. Piao D, Pogue BW, "Rapid near-infrared tomography for hemodynamic imaging using a low coherence wideband light source", *Journal of Biomedical Optics*, Vol. 12, No. 1, pp. 014016-014016-12 (2007).
3. Piao D, Dehghani H, Jiang S, Srinivasan S, and Pogue BW, "Instrumentation for video-rate near-infrared diffuse optical tomography", *Review of Scientific Instruments*, Vol. 76, No. 12, pp. 124301-124301-13 (2005).
4. Piao D, Jiang S, Srinivasan S, Dehghani H, and Pogue BW, "Video-rate near-infrared optical tomography using spectrally-encoded parallel light delivery", *Optics Letters*, Vol. 30, No. 19, Oct. 2005, pp. 2593-2595
5. Dehghani H, Pogue BW, Shudong J, Brooksby B, Paulsen KD. "Three-dimensional optical tomography: resolution in small-object imaging," *Appl Opt.*; Vol. 42, No. 16, pp. 3117-28 (2003).
6. Yalavarthy PK, Dehghani H, Pogue BW, and Paulsen KD, "Critical computational aspects of near infrared circular tomographic imaging: Analysis of measurement number, mesh resolution and reconstruction basis," *Opt. Express* Vol. 14, No. 13, pp. 6113-6127 (2006).

7. **Piao D**, Jiang Z, Xu G, Musgrove C, Bunting CF, Elgawadi A, “Trans-rectal implementation of near-infrared diffuse optical tomography for non-invasive prostate imaging,” Saratov Fall Meetings (SFM) 07, Saratov, Russia, Sep. 25–28, 2007, internet session. (abstract)
8. Eames ME, **Piao D**, Dehghani H, “Source and detector fiber optimization for depth sensitivity in endoscopic near-infrared tomography”, OSA Biomedical Topical Meetings, paper #BSuE30, St. Petersburg, FL, March 16-19, 2008. (3-page paper)

## **APPENDICES**

1. Curriculum vitae
2. Reprints of manuscripts.

## BIOGRAPHICAL SKETCH

NAME <b>Piao, Daqing (Daching)</b>	POSITION TITLE <b>Assistant Professor of Bioengineering</b>		
eRA COMMONS USER NAME			
EDUCATION/TRAINING <i>(Begin with baccalaureate or other initial professional education, such as nursing, and include postdoctoral training.)</i>			
INSTITUTION AND LOCATION	DEGREE <i>(if applicable)</i>	YEAR(s)	FIELD OF STUDY
Tsinghua University, Beijing, China	B.Sc.	1984-1990	Physics
University of Connecticut, Storrs, CT	M.Sc.	1999-2001	Biomedical Engineering
University of Connecticut, Storrs, CT	Ph.D.	2001-2003	Biomedical Engineering

### A. POSITIONS AND HONORS.

#### Positions and Employment

2005--	<b><i>Assistant Professor of Bioengineering</i></b> School of Electrical & Computer Engineering, Oklahoma State University, Stillwater, OK
2004-2005	<b><i>Research Associate</i></b> Thayer School of Engineering, Dartmouth College, Hanover, NH
2003-2004	<b><i>Post-Doctoral Fellow</i></b> Department of Electrical & Computer Engineering, University of Connecticut, Storrs, CT
1994-1999	<b><i>R&amp;D Engineer, Project Manager</i></b> Shanghai Kanglian Medical Engineering Co. Ltd., Shanghai, China
1990-1994	<b><i>MRI Engineer</i></b> Guangdong Weida Medical Apparatus (Group) Co., Guangdong, China

#### Professional Memberships

Member	The Institute of Electrical and Electronics Engineers ( <b>IEEE</b> )
Member	Engineering in Medicine and Biology Society ( <b>EMBS</b> )
Member	The International Society for Optical Engineering ( <b>SPIE</b> )
Member	Optical Society of America ( <b>OSA</b> )

#### Professional Activities

##### ***Journal Paper Reviewer***

2004-	Optics Letters	<b>(Optical Society of America)</b>
2004-	Applied Optics	<b>(Optical Society of America)</b>
2005-	Optical Engineering	<b>(SPIE)</b>
2005-	Journal of Biomedical Optics	<b>(SPIE)</b>
2005-	Lasers in Surgery & Medicine	<b>(American Society for Laser Medicine and Surgery)</b>
2006-	Applied Physics Letters	<b>(American Institute of Physics)</b>
2006-	Expert Review of Medical Devices	<b>(Future Drugs)</b>
2007-	Journal of Selected Topics in Quantum Electronics	<b>(IEEE)</b>
2007-	Optics Express	<b>(Optical Society of America)</b>

##### ***Grant Proposal Reviewer***

2005-	<b><i>Reviewer</i></b> U.S. Civilian Research and Development Foundation Cooperative Research Program
2006-	<b><i>Panelist</i></b> National Science Foundation, CAREER Panel

##### ***Conference Organization***

2008-	<b><i>Session Chair</i></b> SPIE International Symposium on Biomedical Optics (BIOS'08), Conference 6850, Multimodal Biomedical Imaging III, Jan. 19-24, 2008, San Jose, CA.
-------	---

### Awards and Honors

- 1984 **Youngest Freshman of the year** (at the age of 14), Tsinghua University, Beijing, China  
1986 **Electronic Shop Internship Award**, General Electronic Shop, Tsinghua University, Beijing, China (Awarded to 4 out of 100)  
1988 **Machine Shop Internship Award**, General Machine Shop, Tsinghua University, Beijing, China (Awarded to 2 out of 100)  
1989 **Guanghua Prize**, Guanghua Foundation and Tsinghua University, Beijing, China (Awarded to 1 out of 100)  
1990 **magna cum laude**, Tsinghua University, Beijing, China  
1993 **Outstanding Engineer**, Guangdong Weida Medical Apparatus (Group) Corp., Guangdong, China  
2002 **Pre-Doctoral Traineeship Award**, Department of Defense Breast Cancer Research Program  
2003 **Best Ph.D. Thesis Award**, School of Engineering, University of Connecticut, Storrs, CT  
2006 **New Investigator Award**, Department of Defense Prostate Cancer Research Program

### Intellectual Properties

#### **Patent Application**

1. Brian W. Pogue, **Daqing Piao**, "System and method for spectral-encoded high-rate hemodynamic tomography", U.S. patent appl, #20060247531, US Class 600 (2006).
2. Brian W. Pogue, **Daqing Piao**, Keith D. Paulsen, Shudong Jiang, Hamid Dehghani, Heng Xu, Roger Springett, Subha Srinivasan, "Systems and methods for tomographic image reconstruction", World Intellectual Property Organization, patent appl. #PCT/US2006/016210, Class A61B 5/00.

### Invited Professional Talks

- Dartmouth College**, Thayer School of Engineering, Hanover, NH, May 7, 2004  
**Dartmouth Hitchcock Medical Center**, Norris Cotton Cancer Center, Lebanon, NH, Jan. 18, 2005  
**University of Texas Southwestern Medical Center**, BME Program, Dallas, TX, Apr. 7, 2005.  
**University of Texas at Arlington**, Department of Biomedical Engineering, Arlington, TX, Apr. 8, 2005.  
**University of Minnesota**, BME Department and & BME Institute, Minneapolis, MN, Apr. 11, 2005.  
**Oklahoma State University**, School of Electrical & Computer Engineering, Stillwater, OK, Apr. 14, 2005.  
**Marquette University**, Department of Biomedical Engineering, Milwaukee, WI, Apr. 29, 2005.  
**University of Oklahoma**, Bioengineering Center, Norman, OK, Sep. 16, 2005.  
**Nomadics Inc.**, Stillwater, OK, Oct. 26, 2005.  
**Dartmouth College**, Thayer School of Engineering, Hanover, NH, Dec. 12, 2006.  
**University of Connecticut**, Electrical & Computer Engineering Department, Storrs, CT, Dec. 15, 2006.  
**University of Missouri--Columbia**, Department of Biological Engineering, Columbia, MO, Feb. 6, 2007.  
**Washington University in St. Louis**, Department of Biomedical Engineering, St. Louis, MO, Feb. 7, 2007.  
**Siemens Corporate Research**, Division of Imaging and Visualization, Princeton, NJ, Mar. 20, 2007  
**Nomadics Inc.**, Stillwater, OK, July. 25, 2007.  
**The Catholic University of America**, Biomedical Engineering Department, Washington DC, Sep. 17, 2007.

### Invited Conference Presentations

- Saratov Fall Meeting'05**, Saratov, Russia, Sep. 27-30, 2005. Internet invited  
**Saratov Fall Meeting'06**, Saratov, Russia, Sep. 26-29, 2006, Internet invited.  
**SPIE Internal Symposium on Biomedical Optics BIOS'07**, paper 6431-02, San Jose, CA, Jan. 20-25, 2007.  
**SPIE Internal Symposium on Biomedical Optics BIOS'08**, paper 6850-13, San Jose, CA, Jan. 19-24, 2008.

### Other Invited Presentations

- I2E Luncheon----Tulsa**, Tulsa, OK, Nov. 14, 2007, "Featured Innovator"

### Press Coverage

- Research Oklahoma Story, "New method to improve prostate cancer detection," *The Oklahoman*, July 18, 2006.

## B. PUBLICATIONS.

### Book Chapters

- [1] Piao D, "Diffuse Optical Techniques: Instrumentation", a chapter of "*Translational Multimodality Optical Imaging*" Editor: Fred S. Azar and Xavier Intes, Publisher: Artech House. Expected publication by Spring, 2008.

### Journal Papers and Magazine Articles:

#### 2007

- [24] Jiang Z, Zhu Q, and Piao D, "Minimization of geometric-beam-broadening in a grating-based time-domain delay line for optical coherence tomography application," *Journal of Optical Society of America A*, 24(12): 3808-3818 (2007).
- [23] Piao D, Pogue BW, "Rapid near-infrared tomography for hemodynamic imaging using a low coherence wideband light source," *Journal of Biomedical Optics*, 12: 014016 (2007).

#### 2006

- [22] Piao D, Xie H, Zhang W, Kransinski JS, Zhang G, Dehghani H, and Pogue BW, "Endoscopic, rapid near-infrared optical tomography," *Optics Letters*, 31(19): 2876-2878 (2006).
- [21] Piao D, Zhang G, Vemulapalli SN, Dehghani H, Pogue BW, "Near-infrared optical tomography in endoscopy-geometry", *Optics & Photonics News* magazine, 17(12): 31 (2006), "Optics in 2006" special issue.

#### 2005

- [20] Piao D, and Zhu Q, "Direct bi-directional angle-insensitive imaging of the flow signal intensity in Doppler optical coherence tomography," *Applied Optics*, 44(3): 348-357 (2005).
- [19] Chen Y, Otis LL, Piao D, and Zhu Q, "Characterization of dentin, enamel and carious lesions by a polarization-sensitive optical coherence tomography system," *Applied Optics* 44(11): 2041-2048 (2005).
- [18] Piao D, Sadeghi M, Zhang J, Chen Y, Sinusas A., and Zhu Q, "A hybrid positron detection and optical coherence tomography system: Design, calibration and experimental validation with rabbit atherosclerotic models," *Journal of Biomedical Optics*, 10(4): 044010 (2005).
- [17] Piao D, Jiang S, Srinivasan S, Dehghani H, and Pogue BW, "Video-rate near-infrared optical tomography using spectrally-encoded parallel light delivery," *Optics Letters*, 30: 2593-2595 (2005).
- [16] Piao D, Dehghani H, Jiang S, Srinivasan S, and Pogue BW, "Instrumentation for video-rate near-infrared diffuse optical tomography," *Review of Scientific Instruments*, 76: 124301 (2005)

#### 2004

- [15] Piao D, and Zhu Q, "Power-efficient grating-based scanning optical delay line: time-domain configuration," *Electronics Letters*, 40: 97-98 (2004).
- [14] Otis LL, Piao D, Gibson C, and Zhu Q, "Quantifying labial blood flow using optical Doppler tomography," *Oral Surgery, Oral Medicine, Oral Pathology, Oral Radiology, and Endodontics*, 98: 189-194 (2004).
- [13] Yan S, Piao D, Chen Y, and Zhu Q, "Digital signal processor-based real-time optical Doppler tomography system," *Journal of Biomedical Optics*, 9: 454-463 (2004).
- [12] Chen NG, Huang M, Xia H, Piao D, Zhu Q, and Cronin E, "Portable near-infrared diffusive light imager for breast cancer detection," *Journal of Biomedical Optics*, 9: 504-510 (2004).

#### 2003

- [11] Piao D, and Zhu Q, "Quantifying Doppler angle and mapping flow velocity by a combination of Doppler-shift and Doppler-bandwidth measurements in optical Doppler tomography," *Applied Optics*, 42: 5158-5166 (2003).
- [10] Piao D, Otis LL, and Zhu Q, "Doppler angle and flow velocity mapping by combined Doppler shift and Doppler bandwidth measurements in optical Doppler tomography", *Optics Letters*, 28: 1120-1122 (2003).
- [09] Zhu Q, Piao D, Sadeghi M, and Sinusas AJ, "Simultaneous optical coherence tomography imaging and beta particle detection," *Optics Letters*, 28: 1704-1706 (2003).

## 2002

- [08] **Piao D**, Otis LL, Dutta NK, and Zhu Q, "Quantitative assessment of flow velocity estimation algorithms for optical Doppler tomography imaging," *Applied Optics*, 41: 6118-6127 (2002).

## 2001

- [07] **Piao D**, Zhu Q, Dutta NK, Yan S, and Otis LL, "Cancellation of coherent artifacts in optical coherence tomography imaging," *Applied Optics*, 40: 5124-5131 (2001).
- [06] Zhu Q, Chen NG, **Piao D**, Guo P, and Ding X, "Design of near infrared imaging probe with the assistance of ultrasound localization," *Applied Optics*, 40: 3288-3303 (2001).
- [05] Chen NG, Guo P, Yan S, **Piao D**, and Zhu Q, "Simultaneous near infrared diffusive light and ultrasound imaging," *Applied Optics*, 40: 6367-6380 (2001).
- [04] Zhu Q, Chen NG, Guo P, Yan S and **Piao D**, "Near infrared diffusive light imaging with ultrasound localization," *OSA Optics and Photonics News*, 12(12): 31 (2001), Optical Society of America monthly news magazine, "Optics in 2001" special issue.

## 2000

- [03] **Piao D**, and Luo C, "The sparkle noise abatement in RF excitation signal of LMW-400 MRI system," *Chinese Journal of Medical Instrumentation*, 24: 326-329 (2000).

## 1999

- [02] **Piao D**, and Zhou B, "A review on the elimination of MRI acoustic scanning noise," *International Medical Devices*, 5(2): 48-52 (1999), magazine in Chinese.
- [01] Wang Q, Rong L, Lu W, Zhou B, Chen Y, Sun X, and **Piao D**, "The effects of 33.3GHz millimeter wave on H\_(22) liver cancer cell lines and mice model," *Chinese Journal of Gastroenterology*, 4(2), (1999)

### **Conference Proceeding Papers and Abstracts:**

## 2008

- [48] Eames ME, **Piao D**, Dehghani H, "Source and detector fiber optimization for depth sensitivity in endoscopic near-infrared tomography", *OSA Biomedical Topical Meetings*, St. Pittsburg, FL, 2008
- [47] Xu G, Musgrove C, Bunting CF, Dehghani H, **Piao D**, "Sagittal-imaging transrectal optical tomography reconstruction with structural guidance: initial simulative study", *OSA Biomedical Topical Meetings*, St. Pittsburg, FL, 2008.
- [46] Jiang Z, **Piao D**, Elgawadi A, Xu G, "Development of a sagittal-imaging trans-rectal optical tomography probe for coupling with transrectal ultrasound", *OSA Biomedical Topical Meetings*, St. Pittsburg, FL, 2008.
- [45] **Piao D**, "Approach on trans-rectal NIR optical tomography probing for the imaging of prostate with trans-rectal ultrasound correlation", *SPIE International Symposium on Biomedical Optics (BIOS) 08*, # 6850-13, San Jose, CA, January 19-24, 2008 (*invited paper*).

## 2007

- [44] Xu G, Musgrove C, Bunting CF, **Piao D**, "Transrectal optical tomography of prostate with a priori transrectal ultrasound information: initial simulative study", Oklahoma Research Day, Oct. 26, 2007, Edmond, OK.
- [43] **Piao D**, Jiang Z, Zhu Q, "Geometric dispersion effect in a grating-based time-domain optical delay line", Saratov Fall Meetings (SFM) 07, Saratov, Russia, 25-28 September 2007, internet session.
- [42] **Piao D**, Jiang Z, Xu G, Musgrove C, Bunting CF, Elgawadi A, "Trans-rectal implementation of near-infrared diffuse optical tomography for non-invasive prostate imaging," Saratov Fall Meetings (SFM) 07, Saratov, Russia, 25-28 September 2007, internet session.
- [41] **Piao D**, Xie H, Zhang W, Zhang G, Musgrove C, Bunting CF, Dehghani H, Pogue BW, Vemulapalli SN, "Near-infrared optical tomography: endoscopic imaging approach." *SPIE International Symposium on Biomedical Optics (BIOS) 07*, San Jose, CA, January 20-25, 2007 (*invited paper*).
- [40] Xie H, Pogue BW, **Piao D**, "Dual-spectral band continuous wave endoscopic near-infrared optical tomography for hemoglobin and oxygen saturation imaging." *SPIE International Symposium on Biomedical Optics (BIOS) 07*, San Jose, CA, January 20-25, 2007, accepted for oral presentation.

- [39] Musgrove C, Bunting CF, Dehghani H, Pogue BW, **Piao D**, "Computational aspects of endoscopic near-infrared optical tomography: initial investigations." *SPIE International Symposium on Biomedical Optics (BIOS) 07*, San Jose, CA, January 20-25, 2007, accepted for oral presentation.

## 2006

- [38] Xie H, **Piao D**, "Dual-band near-infrared diffuse optical tomography by use of two superluminescent diodes", *Oklahoma Research Day*, Edmond, OK, Dec.1, 2006.
- [37] Jiang Z, **Piao D**, "Multi-modality imaging by a combination of diffuse and coherent optical tomography techniques: initial approach," *Oklahoma Research Day*, Edmond, OK, Dec.1, 2006.
- [36] Piao D, "Hemodynamic imaging by a near-infrared optical tomography system based on a superluminescent diode," *Oklahoma Research Day*, Edmond, OK, Dec.1, 2006.
- [35] **Piao D** "The use of low coherence source for rapid near-infrared diffuse optical tomography and endoscopic near-infrared diffuse optical tomography" *Saratov Fall Meetings (SFM) 06*, Saratov, Russia, 28–30 September 2006 (*invited paper*).
- [34] **Piao D**, Xie H, Zhang W, Zhang G, Musgrave C, Bunting CF, Dehghani H, Pogue BW, "Demonstration of endoscopic near-infrared diffuse optical tomography in phantoms and tissues." *Fifth Inter-Institute Workshop on Optical Diagnostic Imaging from Bench to Bedside at the National Institutes of Health*, Bethesda, MD, 25–27 September 2006, accepted.
- [33] **Piao D**, Jiang S, Dehghani H, Srinivasan S, Pogue BW, "Instrumentation of rapid near-infrared diffuse optical tomography for imaging of tissue at 35 frames per second," *SPIE Photonics West BIOS, SPIE Proceedings* 6081-19, San Jose, CA (2006).
- [32] Xie H, **Piao D**, Pogue BW, Zhang W, "Rapid near-infrared optical tomography by spread-spectral-encoding of single broadband light source," *2006 OSA Biomedical Topical Meetings*, WD9, Fort Lauderdale, FL (2006).
- [31] Pogue BW, **Piao D**, Dehghani H, Paulsen KD, "Demonstration of video-rate diffuse optical tomography in phantoms and tissues," *2006 IEEE International Symposium on Biomedical Imaging*, SU-AM-SS1.2, Arlington, VA (2006).

## 2005

- [30] **Piao D**, Jiang S, and Pogue BW, "Spectral-encoding for parallel source implementation in NIR tomography," *SPIE Photonics West BIOS, SPIE Proceedings* 5693-25, San Jose, CA (2005).
- [29] Zhu Q, **Piao D**, Sadeghi M, Zhang J, Chen Y, and Sinusas A., "A hybrid positron detection and OCT imager," *SPIE Photonics West BIOS, SPIE Proceedings* 5690-60, San Jose, CA (2005).
- [28] Zhu Q, Kurtzman S, Cronin E, Kane M, Huang M, Xu C, Chen NG, **Piao D**, Tannenbaum S, Hedge P, and Jagjivan B, "Benign versus malignant breast masses: optical differentiation using US to guide optical imaging reconstruction," *SPIE Photonics West BIOS, SPIE Proceedings* 5693-56, San Jose, CA (2005).
- [27] Piao D, Dehghani H, Jiang S, Srinivasan S, Pogue BW, "Rapid NIR optical tomography at 35 frames per second by spectrally-encoded parallel light delivery," *Saratov Fall Meetings (SFM) 05*, Saratov, Russia, 27–30 September 2005 (*invited paper*).

## 2004

- [26] Zhu Q, **Piao D**, Sadeghi M, and Sinusas AJ, "Simultaneous optical coherence tomography and beta particle detection," *SPIE Photonics West BIOS, SPIE Proceedings* 5316-55, San Jose, CA, January 2004.
- [25] **Piao D**, and Zhu Q, "Direct bi-directional angle-insensitive flow-intensity detection In Doppler optical coherence tomography," *OSA Biomedical Topical Meetings*, SC8, Miami Beach, Florida (2004).
- [24] **Piao D**, and Zhu Q, "Power-efficient grating-based scanning optical delay line for optical coherence tomography," *OSA Biomedical Topical Meetings*, FH23, Miami Beach, Florida (2004).
- [23] Chen Y, **Piao D**, Otis LL, and Zhu, Q, "Characterization of dentin and enamel by polarization-sensitive optical coherence tomography," *OSA Biomedical Topical Meetings*, FH21, Miami Beach, Florida (2004).

## 2003

- [22] **Piao D**, and Zhu Q, "Accurate estimation of Doppler angler using conventional single-probing-beam optical Doppler tomography," *SPIE Photonics West BIOS, SPIE Proceedings* 4956-39, San Jose, CA (2003).
- [21] Zhu Q, **Piao D**, Sadeghi M, and Sinusas AJ, "Simultaneous optical coherence tomography and beta particle detection," *SPIE Photonics West BIOS, SPIE Proceedings* 5316-55, San Jose, CA (2003).
- [20] Yan S, **Piao D**, and Zhu Q, "A DSP-based optical Doppler tomography system for real-time signal processing," *SPIE Photonics West BIOS, SPIE Proceedings* 4956-33, San Jose, CA (2003).
- [19] Chen NG, **Piao D**, Xia H, and Zhu Q, "Portable multi-channel multi-wavelength near infrared diffusive light imager," *SPIE Photonics West BIOS, SPIE Proceedings* 4955-25, San Jose, CA (2003).

## 2002

- [18] **Piao D**, Albreski D, and Zhu Q, "Preliminary results of imaging and diagnosis of nail fungal infection with optical coherence tomography," *Technical Digest of OSA Biomedical Topical Meetings*, 65-68, Miami Beach, Florida (2002).
- [17] **Piao D**, Zhu Q, and Otis LL, "Optical Doppler coherent tomography algorithms: quantitative analysis," *Proceedings of IEEE International Symposium on Biomedical Imaging*, 293-296, Washington D.C. (2002).
- [16] Huang M, Xie T, Chen NG, **Piao D**, and Zhu Q, "2-D NIR imaging reconstruction with ultrasound guidance," *Proceedings of IEEE International Symposium on Biomedical Imaging*, 1031-1034, Washington D.C. (2002).

## 2001

- [15] **Piao D**, Zhu Q, Dutta NK, Yan S, and Otis LL, "Cancellation of coherent artifacts in OCT image," *SPIE Photonics West BIOS, SPIE Proceedings* 4251-04, San Jose, CA (2001).
- [14] Zhu Q, Chen NG, Guo P, Yan S, and **Piao D**, "Design of combined ultrasound and near infrared diffusive-light imaging probe," *SPIE Photonics West BIOS, SPIE Proceedings* 4256-31, San Jose, CA (2001).
- [13] Zhu Q, Guo P, Chen NG, Yan S, and **Piao D**, "Clinical evaluation of simultaneous ultrasound and NIR imaging," *SPIE Photonics West BIOS, SPIE Proceedings* 4250-68, San Jose, CA (2001).
- [12] **Piao D**, Chen NG, Zhu Q, Dutta NK, and Otis LL, "Imaging of fluid flow velocity using Doppler optical coherence tomography: preliminary results," *Proceedings of the IEEE 27th Annual Northeast Bioengineering Conference*, 55-56, Storrs, CT (2001).
- [11] **Piao D**, Zhu Q, Dutta NK, Yan S, and Otis LL, "Coherent artifacts in optical coherence tomography: observation and cancellation," *Proceedings of the IEEE 27th Annual Northeast Bioengineering Conference*, pp. 53-54, Storrs, CT, March/April 2001.
- [10] Otis LL, **Piao D**, Zhu Q, Dutta NK, and Yan S, "The effect of source power on image clarity in optical coherence tomography," *AADR/CADR Annual Meeting*, Chicago, IL, *Journal of Dental Research*, 80: 694 (2001).

## 2000

- [09] Zhu Q, Chen NG, Guo P, Yan S, **Piao D**, "Combined ultrasound and near-infrared diffuse light imaging", *IEEE International Ultrasonics Symposium*, San Juan - Puerto Rico October 22-25, 2000.
- [08] **Piao D**, Ding X, Guo P, and Zhu Q, "Optimal distribution of near infrared sensors for simultaneous ultrasound and NIR imaging," *Technical Digest of OSA Biomedical Topical Meetings*, 472-474, Miami Beach, Florida (2000).
- [07] **Piao D**, Zhu Q, Dutta NK, and Otis LL, "Effect of source coherence on interferometric imaging," *Technical Digest of OSA Biomedical Topical Meetings*, 145-147, Miami Beach, Florida (2000).
- [06] Ding X, **Piao D**, and Zhu Q, "Optimal design of near infrared imaging probe in reflection geometry," *Technical Digest of OSA Biomedical Topical Meetings*, 438-440, Miami Beach, Florida (2000).
- [05] Guo P, Zhu Q, **Piao D**, Fikiet J, and BenOmran A, "Combined ultrasound and NIR imager," *Technical Digest of OSA Biomedical Topical Meetings*, 97-99, Miami Beach, Florida (2000).
- [04] **Piao D**, Ding X, Guo P, Yan S, and Zhu Q, "Effects of near infrared sensor distribution upon reconstructed optical properties of simultaneous ultrasound and NIR imaging", *Proceedings of the IEEE 26th Annual Northeast Bioengineering Conference*, pp. 93-94, Storrs, CT, April 2000

- [03] **Piao D**, Zhu Q, Dutta NK, Yan S, and Otis LL, "Effect of source coherence on low coherence interferometric imaging," Proceedings of the IEEE 26th Annual Northeast Bioengineering Conference, pp. 91-92, Storrs, CT, April 2000.
- [02] Guo P, **Piao D**, Zhu Q, and Fikiet J, "A combined 2-D ultrasound and NIR imaging system," Proceedings of the IEEE 26th Annual Northeast Bioengineering Conference, pp. 77-78, Storrs, CT, April 2000.
- [01] Ding X, **Piao D**, and Zhu Q, "Optical imaging array design with multiple sources and detectors," Proceedings of the IEEE 26th Annual Northeast Bioengineering Conference, pp. 69-70, Storrs, CT, April 2000.

## C. RESEARCH SUPPORT

### Ongoing Research Grant

<b>1. DOD CDMRP PC060814</b>	<b>Piao, D. (PI)</b>	<b>03/01/2007 – 02/28/2010</b>	<b>\$306,238</b>
		<b>OSU-CEAT matching fund</b>	<b>\$25,000</b>

Department of Defense—Prostate Cancer Research New Investigator Award  
 "Transrectal Near-infrared Tomography for Prostate Imaging"

The goal of this study is to develop and validate trans-rectal near-infrared optical tomography technique for *in vivo* prostate cancer imaging and targeted biopsy guidance.

#### **Co-PIs:**

Dr. Charles F. Bunting, School of Electrical and Compute Engineering, Oklahoma State University  
 Dr. Sreenivas N. Vemulapalli, Department of Urology, University of Oklahoma Health Science Center.

<b>2. OCAST HR-06-171S</b>	<b>Piao, D. (PI)</b>	<b>09/01/2006 – 08/31/2009</b>	<b>\$135,000</b>
----------------------------	----------------------	--------------------------------	------------------

Oklahoma Center for the Advancement of Science and Technology  
 "Video-rate endoscopic NIR tomography of hemodynamics"

The goal of this study is to develop an innovative imaging technology that may benefit *in vivo* non-invasive detection of cancer in internal organs by assessing hemodynamics in real-time.

#### **Co-PIs:**

Dr. Brian W. Pogue, Thayer School of Engineering, Dartmouth College  
 Dr. Guolong Zhang, Department of Animal Sciences, Oklahoma State University

### Completed Research Grant

<b>DAMD17-02-1-0358</b>	<b>Piao, D. (PI)</b>	<b>06/15/02 – 06/14/05</b>	<b>\$65,994</b>
-------------------------	----------------------	----------------------------	-----------------

Department of Defense US Army Medical Research and Materiel Command (USAMRMC)  
 "Monitoring cancer oxygenation changes induced by ultrasound"

The goal of this study was to evaluate a new hypothesis that oxygen delivery to the localized tumor region could be enhanced by ultrasound at the diagnostic radiation level.

### Proposal in Preparation

Proposal Pending

Proposal Declined

# Source and detector fiber optimization for depth sensitivity in endoscopic near infrared tomography

Matthew E Eames<sup>1</sup>, Daqing Piao<sup>2</sup> and Hamid Dehghani<sup>1</sup>

<sup>1</sup>*School of Physics, University of Exeter, UK*

<sup>2</sup>*School of Electrical and Computer Engineering, Oklahoma State University, OK 74078, USA  
email:h.dehghani@exeter.ac.uk, Tel:+44 1392 264177, Fax:+44 1392 261111*

**Abstract:** NIR optical tomography in endoscopic imaging geometry is a novel technique for non-invasive tissue-specific cancer detection in internal organs. The arrangement of source and fiber detection system is an important aspect in maximizing depth sensitivity in particular for axial imaging. This study demonstrates that using multiple arrays of fibers within an elliptic shaped probe increases depth resolution as compared to single array of fibers within a cylindrical shaped probe.

©2008 Optical Society of America

**OCIS codes:** (170.6960) Tomography; (100.3010) Image reconstruction techniques; (100.3190) Inverse problems

## 1. Introduction

Near-infrared (NIR) optical tomography is a non-invasive functional imaging technique that has shown the potential of acquiring unique tissue-specific functional contrast by using tomographic measurement of NIR attenuation within tissue. The high contrast of NIR optical tomography originates from the stronger light attenuation of hemoglobin relative to water in parenchymal tissue at the 650-900 nm range, as well as the distinct spectral differences of hemoglobin between the oxygenated and deoxygenated states. Contrast as high as 300 percent has been demonstrated in NIR tomography for vascular densities of only 2 percent [1]. Such high blood-based contrast allows pathognomic diagnosis of increased vascularity in malignant tissues and hemodynamic imaging of tissue function and physiology.

Over the past two decades, NIR optical tomography has been advanced steadily by investigating and clinical testing of key applications in the characterization of breast cancer [2], the assessment of brain functionality [3] and the evaluation of extremity abnormality [4]. The majority of applications to date have focused on using external applicator arrays. Specifically, most applications have used a method by which NIR light is directed into tissue using optical fibers at the external surface of the imaging volume and measuring the emitting light at other points on the same surface using either separate fibers or a non-contact imaging detector array. The potential of imaging internal organs like prostate has driven the growing interest that extends NIR optical tomography to endoscopic or transrectal geometries. The key factor in attempting NIR tomography of internal organs has been the development of appropriate applicator arrays. Recently, novel applicator array was constructed and demonstrated as an NIR optical tomography system that allows two dimensional (2D) NIR contrast mapping of internal organs using a non-invasive internal interrogation [5]. The technique incorporates a broadband light source with spectrometer-based detection. The broadband light that disperses with a grating and passes a collimating lens forms a one-dimensional linear distribution of the source spectrum, which is coupled to the tissue by linearly aligned fibers. The fibers are arranged into a circular geometry inside an endoscope probe, Figure 1(a) and (b), where either a coated cone prism or a set of microoptics assembly is used for circumferential light deflection. The wavelength separation coupled to each fiber generates spread-spectral-encoding of the illumination over to the tissue, which accommodates concurrent sampling of all source-detector pairs when using a spectrometer and CCD in the detection. This design enables both the probing in transrectal geometry and the rapid sampling for NIR optical tomography.

Imaging in trans-rectal geometry gives little flexibility to the placement of optodes when axial imaging is aimed for. Little work has been done to investigate the optimum arrangement of the optodes for the excitation and detection of the NIR signal, within the compact transrectal geometry. The current method uses a cylindrical design with 8 sources and 8 detectors placed uniformly around a single ring of the probe, Figure 1. Upon the excitation of tissue using the sources (*S* in Figure 1(b)), measurements are made at all 8 detectors, simultaneously, to reconstruct cross-sectional images of optical perturbations within the region being imaged. One limitation that may exist with this 2D single plane measurement scheme is in the depth resolution and sensitivity. It is therefore important to investigate the merits and benefits of using multiple plane source and detection arrays, mounted within the cylindrical probe to assess any improvement possible in depth sensitivity of the measured signal.

## BSuE30.pdf

In this work, sensitivity analysis of multiple detection systems in terms of increasing the number and configuration of source / detect arrangements will be investigated for the current cylindrical probe, in three dimensions (3D) as well as exploring the use of non-cylindrical, elliptic probe designs that may offer alternative improvements in depth resolution.

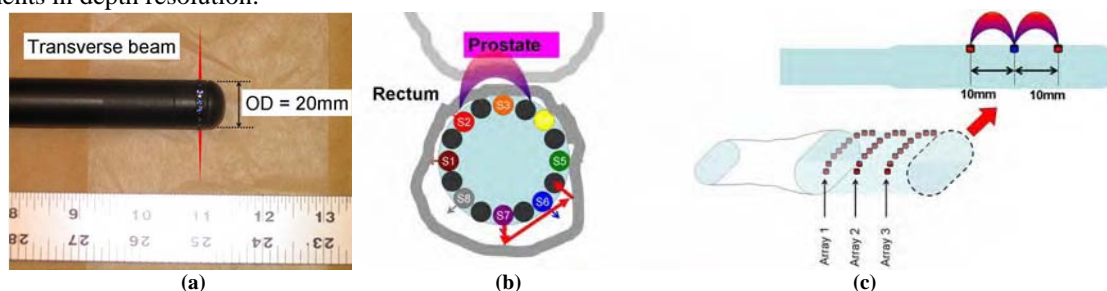


**Figure 1.** (a) The cylindrical transrectal probe and (b) 2D cross-section showing the source and detector arrangements. (c) proposed elliptical probe design consisting of either a single layer of source and detectors in a single array, or two array of detectors with a single array of sources in between.

## 2. Methods

The first probe design cylindrical shape is shown in Figure 1(a) and (b). This probe is modeled as a cylinder of length 40mm ( $-20\text{mm} \leq z \leq 20\text{mm}$ ) with inner radius 10mm and outer radius 20mm. Two different data collection strategies are considered: (a) 8 sources and 8 detectors distributed evenly in a single ring of fibers at  $z = 0$  mm and (b) three separate rings of 8 sources and 8 detectors, at  $z = 0$  mm, 10 mm and -10 mm. In this case, the depth of tissue modeled as surrounding the probe is set at 10 mm. This design is better suited for imaging through a lumen that can enclose the probe completely without much airgap between the probe surface and surrounding tissue.

The second probe design, shown in Figure 1(c) is an elliptical shaped probe. The probe is an elliptical cylinder of length 40mm ( $-20\text{mm} \leq z \leq 20\text{mm}$ ) with major radius 20mm and minor radius 10mm surrounded by a cylindrical mesh of radius 30mm. This design of placing the arrays of sources and detectors on just one side of the probe is better fitted to imaging prostate through rectal wall. The three arrays have a longitudinal separation of 10mm and placed along the minor axes at positions  $z = -10$  mm,  $z = 0$  mm and  $z = 10$  mm about  $x = 0$  mm. Two different data collection strategies are considered: (a) 5 sources and 4 detectors interleaved in a single line (Array 2 in Figure 1(c)), and (b) three separate rings of 8 sources (Array 2) at  $z=0$ mm and 8 detectors (Array 1 and 3) at  $z = 10$  mm and -10 mm. In this case, the depth of tissue modeled as surrounding the probe is set at 20 mm in the short axis and 10 mm in the long axis. The angular separation of each channel in both cases is  $8^\circ$ . The accuracy of diffusion approximation can be maintained for array setup of (b), while it may be comprised in array setup of (a).

To simulate the propagation and hence the sensitivity of the NIR signal throughout the volume of interest, a finite element model is used for each probe design. The propagation of light within the surrounding tissue was calculated using the diffusion approximation and the total sensitivity of intensity data to absorption changes within the model, for all source and detector combination was calculated.

## 3. Results

The normalized total sensitivity of each probe design and fiber arrange strategy is shown in Figure 2. Note that for the cylindrical case the depth of tissue modeled as surrounding the probe is set at 10 mm, where as in the elliptic case the depth of tissue modeled as surrounding the probe is set at 20 mm in the short axis and 10 mm in the long axis. It is evident that by the use of a single array of fibers, the total sensitivity of measured intensity data to small changes in absorption rapidly decays as a function of distance away from the source and detector array. In each of the models, the maximum sensitivity is seen directly above the detector fibers and for the elliptical probe, the sensitivity is more uniform within the tissue being sampled.

In order to evaluate the increase in depth sensitivity, the cross sectional profile of the sensitivity as a function of depth was calculated for each of the models and is shown in Figure 3. It is seen that the use of multiple fiber arrays improves the depth sensitivity of both probe designs, with the greater depth seen using the elliptical probe. The use of elliptical probe with a single detection array does not provide additional depth sensitivity, whereas the addition of multiple arrays to the elliptical probe, not only increased the depth sensitivity, but also provides a more uniform sensitivity at lower decay rate as a function of depth.

## 4. Discussion

In this paper we have shown that for axial imaging geometry the use of an elliptic shaped probe together with 3 arrays of detection system improves the depth sensitivity of measured intensity signal to absorption changes

within the tissue being sampled. This increased sensitivity is crucial when designing a non-invasive axial imaging probe for endoscopic NIR tomography imaging of internal organs such as the prostate to detect and characterize abnormal lesions.

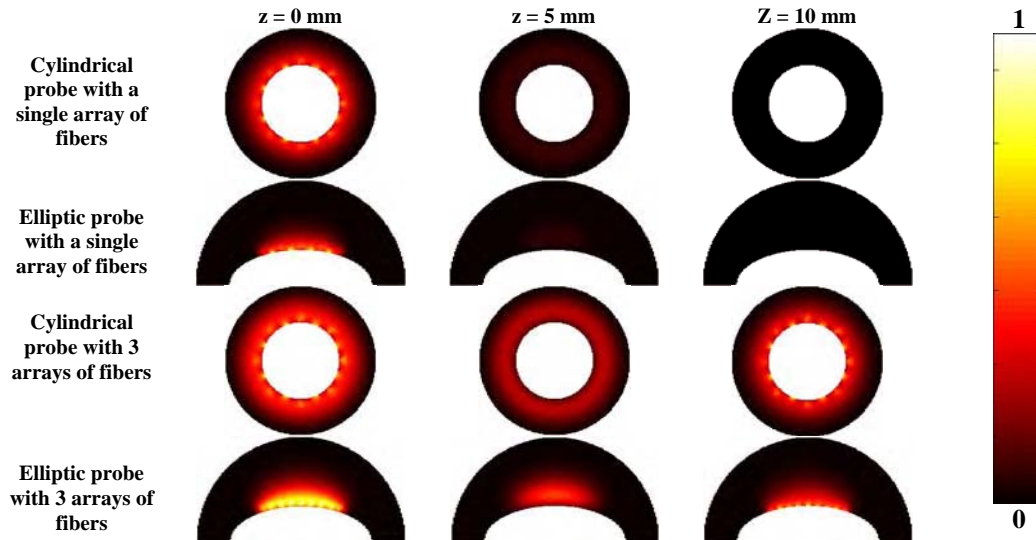


**Figure 2.** The normalized sensitivity of each probe design and fiber arrangement strategy. The images presented are coronal cross-sections of the 3D model at different sections. Note that for the cylindrical case the depth of tissue modeled as surrounding the probe is set at 10 mm, where as in the elliptic case the depth of tissue modeled as surrounding the probe is set at 20 mm in the short axis and 10 mm in the long axis.

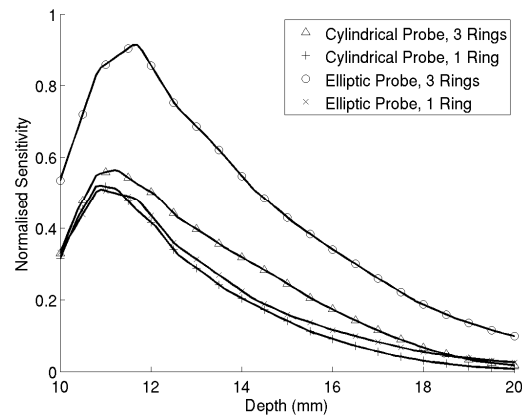


**Figure 3.** Cross sectional normalized sensitivity profile for each probe design as a function of depth

## 5. Acknowledgements

This work has been partially supported by Congressionally Directed Medical Research Program through grant PC060814.

## 6. References

- Pogue, B.W., Poplack, S. P., McBride, T. O., Wells, W. A., Osterman K. S., Osterberg, U. L., Paulsen, K. D., *Quantitative Hemoglobin Tomography with Diffuse Near-Infrared Spectroscopy: Pilot Results in the Breast*. Radiology, 2001. **218**(1): p. 261-6.
- Srinivasan, S., Pogue, B. W., Jiang, S., Dehghani, H., Kogel, C., Soho, S., Gibson, J. J., Tosteson, T. D., Poplack, S. P., Paulsen, K. D., *Interpreting Hemoglobin and Water Concentration, Oxygen Saturation and Scattering Measured In Vivo by Near-Infrared Breast Tomography*. PNAS, 2003. **100**(21): p. 12349-12354.
- Zeff, B.W., White, B. R., Dehghani, H., Schlaggar, B. L., and Culver, J. P., *Retinotopic mapping of adult human visual cortex with high-density diffuse optical tomography*. PNAS, 2007. **104**: p. 12169-12174.
- Scheel, A.K., Backhaus, M., Klose, A. D., Moa-Anderson, B., Netz, U. J., Hermann, K. A., Beuthan, J., Müller, G. A., Burmester, G. R. and Hielscher, A. H., *First clinical evaluation of sagittal laser optical tomography for detection of synovitis in arthritic finger joints* Annals of the Rheumatic Diseases, 2005. **64**: p. 239-245.
- Piao, D., Xie, H., Zhang, W., Krasinski, J., Zhang, G., Dehghani, H. and Pogue, B. W., *Endoscopic, rapid near-infrared optical tomography*. Optics Letters, 2006. **31**(9): p. 2876-2878.